(19) U. Jentschura and E. Lippert, *Ber. Bunsenges. Phys. Chem.*, **75**, 782 (1971).
(20) F. Thyrion and D. Decroocq, *C.R. Acad. Sci. (Paris)*, **260**, 2797 (1965).
(21) W. B. Person, *J. Am. Chem. Soc.*, **87**, 167 (1965).
(22) D. A. Deranleau, *J. Am. Chem. Soc.*, **91**, 4044, 4050 (1969).
(23) T. Higuchi and K. A. Connors, *Adv. Anal. Chem. Instrum.*, **4**, 117 (1965).
(24) B. D. Anderson, J. H. Rytting, and T. Higuchi, *J. Pharm. Sci.*, **69**, 676 (1980).
(25) S. S. Davis, T. Higuchi, and J. H. Rytting, *Adv. Pharm. Sci.*, **4**, 73 (1974).
(26) J. J. Christensen, M. D. Slade, D. E. Smith, R. M. Izatt, and J. Tsang, *J. Am. Chem. Soc.*, **92**, 4164 (1970).
(27) O. Levy, G. Y. Markovits, and I. Perry, *J. Phys. Chem.*, **79**, 239 (1975).

ACKNOWLEDGMENTS

This study was supported in part by The Atkinson Charitable Foundation and by the Medical Research Council of Canada, to whom we express our thanks. The authors also thank Mr. Joseph Go for skilled technical assistance and Mrs. Vivienne Hinds for typing the manuscript.

pH–Solubility Profile of Papaverine Hydrochloride and Its Relationship to the Dissolution Rate of Sustained-Release Pellets

ABU T. M. SERAJUDDIN ˣ and MORTON ROSOFF*

Received January 28, 1983, from the *Pharmacy Research and Development Department, Research and Development Division, Revlon Health Care Group, Tuckahoe, NY 10707.* Accepted for publication August 16, 1983. *Present address: Arnold and Marie Schwartz College of Pharmacy and Health Sciences, Brooklyn, NY 11201.

Abstract □ The pH–solubility profile of papaverine hydrochloride (I) was determined using the phase-solubility technique and equilibrium solubilities in buffers. The release of I from sustained-release pellets consisting of a shellac-based matrix was determined by the USP basket technique and was found to exhibit zero-order kinetics. Release rates at various pH values of the permeating solvent were compared with the pH–solubility profile and were directly proportional to the solubility below, but not above, the apparent pH_{max} (3.9). This lack of proportionality was also shown by the intrinsic dissolution rates. The effect was attributed to the self-buffering action of I and the metastability of the papaverine salt–base system in the vicinity of pH_{max}. It is postulated that the outer layer of polymer and filler on the surface of the pellets forms a barrier which determines the rate of release. The inner matrix serves as a drug reservoir in which the internal pH may not be the same as the bulk pH.

Keyphrases □ Papaverine hydrochloride—pH–solubility profile, supersaturation effect, common-ion effect, solubility–dissolution rate ratio, self-buffering effect □ Shellac-based matrix—sustained-release dosage forms, solubility–dissolution rate ratios, internal self-buffering effect □ Mechanism of release—matrix model, effect of filler

The solubility of a hydrochloride salt and its base may vary greatly in the GI pH range, depending on the solubilities of ionized and un-ionized forms and the pK_a of the compound (1). Kramer and Flynn (2) have investigated the solubility interrelationships of hydrochloride salts and their bases. They observed that instead of giving a smooth curve, the solubility curves of a salt and its base intersect at a sharp angle at the pH of maximum solubility (pH_{max}) of both forms. Chowhan (3) has also noticed a similar relationship between organic acids and their salts.

The release of papaverine hydrochloride (I) from commercial sustained-release preparations has been reported to be significantly affected by pH (1). A partial pH–solubility profile showed that the drug solubility reached a maximum at pH ~4.5, and a common-ion effect owing to the addition of excess chloride ion was noticed at low pH.

In the present investigation, the pH–solubility profile of I and the interrelationships betwen the solubility of its salt and base forms were studied. Experiments were then conducted to study the dissolution of I from sustained-release pellets[1] in relation to the pH–solubility profile.

EXPERIMENTAL SECTION

Materials—Papaverine hydrochloride[2] (I) was used as received. The papaverine base (II) was prepared by increasing the pH of an aqueous solution of I to at least 12.0, washing the resultant precipitate four to five times with water, and drying under reduced pressure over phosphorus pentoxide. The identity of II was established by elemental analysis.

Commercial sustained-release papaverine hydrochloride capsules were used as the dosage forms. Each capsule contained ~500 pellets. The diameter of each individual pellet was 0.9 ± 0.1 mm. The diameter of sugar granules around which I was embedded in a shellac-based matrix by a coating process in a conventional rotating pan (4) was ~0.6 mm. The outermost layers of pellets were formed by the addition of drug-free shellac and filler.

The citric acid–phosphate buffers (pH 2.2–7.8) were prepared by mixing 0.1 M citric acid and 0.2 M disodium phosphate. All other reagents used were of analytical grade.

pH–Solubility Profile—The solubility profile of I and its base was determined by the phase-solubility technique of Dittert *et al.* (5). The pH of I in saturated aqueous solution was 3.0. The solubilities at pH <3.0 were determined by titrating dropwise with 1 M HCl, stirring with an overhead stirrer for 1 h at 37°C in a water bath, recording the pH, and then collecting a suitable aliquot. To attain a higher pH, 1 M NaOH was similarly added. Throughout the titration, care was taken to maintain an excess of solid in equilibrium with the solution. The aliquots were filtered[3] immediately, diluted with 0.1 M HCl, and analyzed spectrophotometrically[4] at 310 nm. The solubility was calculated in terms of the hydrochloride salt. A preliminary study showed that the solubility did not change significantly if the equilibration of solution was continued for more than 1 h after each addition of titrant.

The solubility in a citric acid–phosphate buffer was determined by adding an excess of I to ~15 mL of the buffer in a 50-mL volumetric flask, shaking overnight with a wrist-action shaker[5] in a water bath at 37°C, and analyzing the aliquot as described above. The saturation solubility in 0.01 and 0.1 M HCl was determined in the same manner.

[1] Cerespan, (lot no. 56370; 150 mg); USV Pharmaceutical Corp., Tuckahoe, N.Y.
[2] USVP no. 29745; USV Pharmaceutical Corp., Tuckahoe, N.Y.
[3] Millipore filter, Type HA; Millipore Corp., Bedford, Mass.
[4] Model 25; Beckman Instruments, Fullerton, Calif.
[5] Burrell Corp., Pittsburgh, Pa.

0022-3549/84/0900-1203$01.00/0

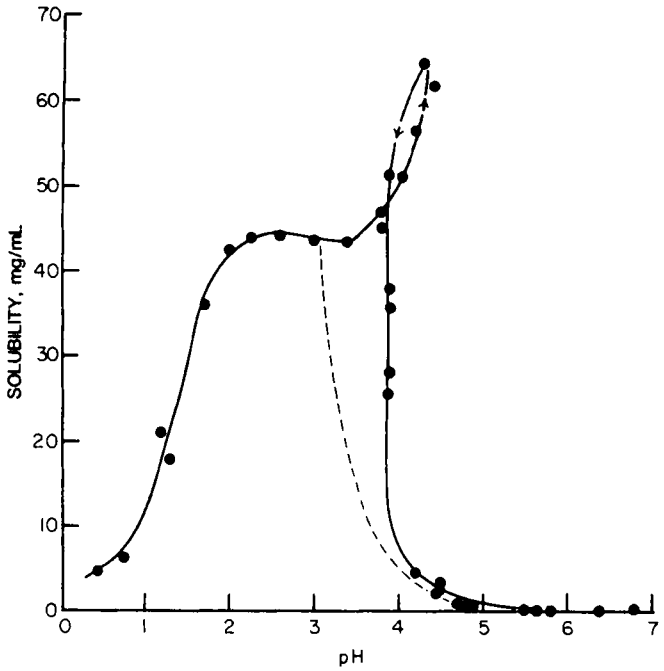

Figure 1—*Solubility of I in water at 37°C as a function of pH determined by adjusting the pH with 1 M HCl at pH <3.0 or with 1 M NaOH at pH >3.0. Each point represents one experimental value. All data were calculated in terms of hydrochloride salt equivalent. The broken line shows the theoretical solubility profile according to Eq. 3.*

The pH of the buffers with initial values >4 shifted to lower values on addition of I; consequently, the solubilities at these pH values were determined by using II, which gave no significant change in pH. The pH values of 0.01 and 0.1 M HCl media remained practically unchanged in the presence of I.

Analysis of Chloride Ion—During the determination of the solubility of I by the addition of 1 M HCl or 1 M NaOH, the analysis of chloride ion was made with selected aliquots. For the determination of chloride concentration, the aliquots were diluted 50 or 100 times with water, and 2 mL of 5 M $NaNO_3$ for each 100 mL of the diluted solution was added. The electrode potential in millivolts was measured with a pH meter[6] fitted with a chloride-sensitive electrode[7]. The standard calibration curve of log $[Cl^-]$ *versus* millivolts was obtained with sodium chloride solutions containing 2 mL of 5 M $NaNO_3$/100 mL.

Determination of pK_a—The apparent pK_a values of papaverine reported in the literature are 5.95 (6), 6.95 (7), and 6.40 (8). Since variations were noticed, the pK_a was determined in this study by recording the UV spectra of 0.015-mg/mL solutions of I in citric acid–phosphate buffer under various pH conditions. The average pK_a value obtained from the absorbances at 310 nm, using the following equation, was 6.5:

$$pK_a = pH - \log\left[\frac{A_{obs} - A_{BH^+}}{A_B - A_{obs}}\right] \qquad \text{(Eq. 1)}$$

where A_{BH^+} and A_B are the absorbances of the ionized and un-ionized species, respectively, and A_{obs} is the observed absorbance at the particular pH.

Dissolution from Papaverine Sustained-Release Pellets—A method using the USP dissolution apparatus[8] was developed for measuring the dissolution rates of papaverine hydrochloride-containing pellets. The contents of one capsule were placed in a dissolution basket, and the basket was immersed in 900 mL of dissolution medium previously warmed to 37°C. The basket was rotated at 100 rpm, and aliquots were taken from a point near the upper end of the basket and midway between the cylindrical edge of the basket and the wall of the vessel. The aliquots were analyzed spectrophotometrically at 310 nm, and the concentrations of the drug were determined from the extinction coefficients at the particular pH.

Intrinsic Dissolution of I—The intrinsic dissolution rates of I were determined using the dissolution apparatus described by Wood *et al.* (9). About 700 mg of the sample was compressed in a die with a hydraulic press[9] at a pressure of 4540 kg. The assembly was immersed in 300 mL of the medium at 37°C and stirred at 220 rpm. The surface of the pellet exposed to buffer had an area of 0.95 cm^2. The drug was assayed by removing suitable aliquots, diluting with 0.1 M HCl, and reading the absorbance spectrophotometrically at 310 nm.

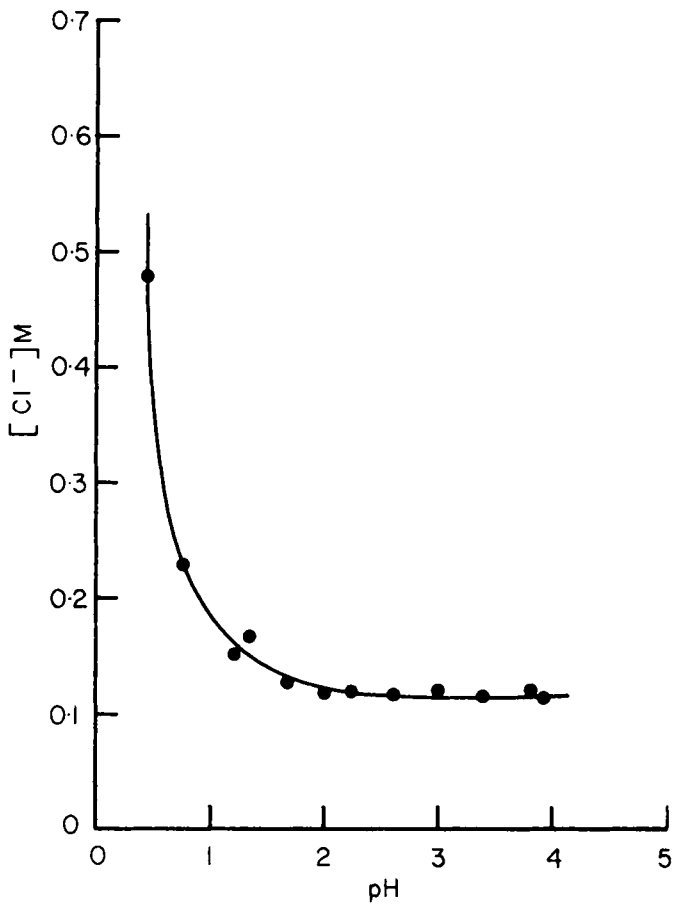

Figure 2—*The concentrations of chloride ion in the saturated solutions of I plotted as a function of pH (pH < apparent pH_{max}).*

Determination of the Effect of I on the pH of Buffers—The change in buffer pH in contact with I was determined in two ways. First, the citric acid–phosphate buffer, with pH 5, 6, or 7, was added to 1 g of I and stirred with a magnetic stirrer. The pH was recorded when stabilized, after the addition of 4 mL of the buffer and after 2-mL additions. Alternatively, the solid form of I was added in 0.1-g aliquots to 50 mL of a pH 6 buffer. The stabilized pH was recorded after each addition of solid.

Photomicroscopy of the Cross Sections of Pellets—The pellets were embedded in paraffin, and sections at a thickness of 10 μm were cut with a rotary microtome[10] using a diamond knife. The midsections of pellets were affixed to glass slides with egg albumin, and photomicrographs[11] were taken under UV light.

Determination of Density and Porosity—The densities of I and the sustained-release pellets were measured with a null pycnometer[12] using helium gas. Helium was purged through the samples for 12–15 min at the rate of 2–3 bubbles/s prior to the density measurement. The porosity of the pellets was determined by a mercury intrusion porosimeter[13].

RESULTS AND DISCUSSION

Solubility of I—The solubility of I at 37°C as a function of pH determined with the salt is shown in Fig. 1. It is observed from this figure that supersaturated solutions with a pH between 3.9 and 4.5 were formed; the pH of the supersaturated solution rose to 4.5 with the addition of 1 M NaOH before the precipitation of papaverine base (II) ensued; the pH finally stabilized at 3.9 (apparent pH_{max}). Elemental analysis of the solid phase precipitating at pH

[6] Digital 110; Corning Instruments, Medfield, Mass.
[7] Model 96-17; Orion Research, Cambridge, Mass.
[8] Model 72-RL; Hanson Research, Northridge, Calif.
[9] Fred S. Carver; Inc., Monomonee Falls, Wis.
[10] Model 820; American Optical Corp., Buffalo, N.Y.
[11] Series 10 microscope; American Optical Corp.
[12] Model PY-5; Quantachrome Corp., Syosset, N.Y.
[13] Model J5-7125D; American Instrument Co., Silver Spring, Md.

Table I—Dissolution Rates from Sustained-Release Pellets, Intrinsic Dissolution Rates, and Ratios of Rates to Solubilities of Papaverine Hydrochloride at Various pH Values

Medium	pH_{bulk}	Solubility of I at pH_{bulk} at 37°C	Dissolution Rate from Pellets, mg/min	Ratio of Dissolution Rate from Pellets to Solubility	Intrinsic Dissolution Rate of I, $mg \cdot cm^{-2} \cdot min^{-1}$	Ratio of Intrinsic Dissolution Rate to Solubility
0.1 M HCl	1.1	19.9	0.6	0.030	2.6	0.131
0.01 M HCl	2.0	42.1	1.6	0.038	6.3	0.150
Citric Acid-Phosphate Buffer	2.2	62.0	2.3	0.037	10.2	0.163
	3.0	60.5	2.5	0.041	—	—
	4.0	62.5	2.5	0.040	9.8	0.157
	5.0	0.41	2.2	5.4	9.0	22.0
	5.4	0.16	1.1	6.9	—	—
	6.0	0.047	0.24	5.1	4.1[a]	87.2
	7.0	0.016	0.11	6.9	—	—

[a] Rate may have been affected by the deposition of a porous film on the dissolving surface.

3.9 revealed that the solid consisted of II only. The applicable equations (2) to express the total solubility (S_T) of salt and base at any pH are:

$$S_{T(pH < pH_{max})} = [BH^+]_s + [B] = [BH^+]_s\left(1 + \frac{K_a}{[H_3O^+]}\right) \quad \text{(Eq. 2)}$$

$$S_{T(pH > pH_{max})} = [BH^+] + [B]_s = [B]_s\left(1 + \frac{[H_3O^+]}{K_a}\right) \quad \text{(Eq. 3)}$$

where $[BH^+]$ and $[B]$ are the concentrations of the ionized and un-ionized species, respectively. The subscripts $pH < pH_{max}$ and $pH > pH_{max}$ indicate that the equations are applicable for pH values less than and greater than pH_{max}, respectively. The subscripts indicates a saturated species, and K_a is the apparent dissociation constant. Each of these equations describes an independent curve limited by the solubility of one of the two species, and pH_{max} is the juncture of the two curves. The solid phases in equilibrium with the solutions at a pH lower or higher than the pH_{max} are salt and base, respectively. By using the apparent pK_a of 6.5 and a solubility of 0.015 mg/mL for the base, the theoretical curve corresponding to Eq. 3 is also drawn in Fig. 1. The experimental values agree with Eq. 3 only at a pH >4.6. Below this pH, the experimental points are higher than the theoretical line, and the calculated pH_{max} (3.0) is lower than the apparent value (3.9).

The supersaturation at pH values of 3.9–4.5 in Fig. 1 is released by nucleation when the pH shifts to either side of the apparent pH_{max}. This was proven by the rapid precipitation observed when a supersaturated solution of salt was nucleated with solid base or *vice versa*.

According to Eq. 2, the total solubility below pH_{max} should remain constant,

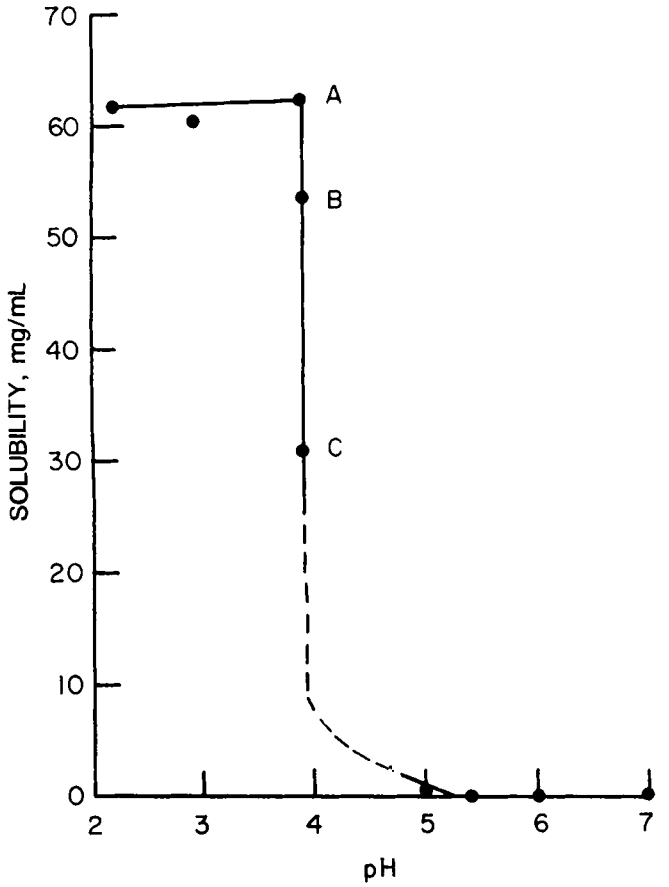

Figure 3—*The solubility of I in citric acid-phosphate buffers. A, B, and C were obtained when an excess of I was added to buffers of pH 4.0, 5.0, and 5.4, respectively. The solubility at pH ≥5 was determined with II. Each point represents one experimental value. All data were calculated in terms of hydrochloride salt equivalent.*

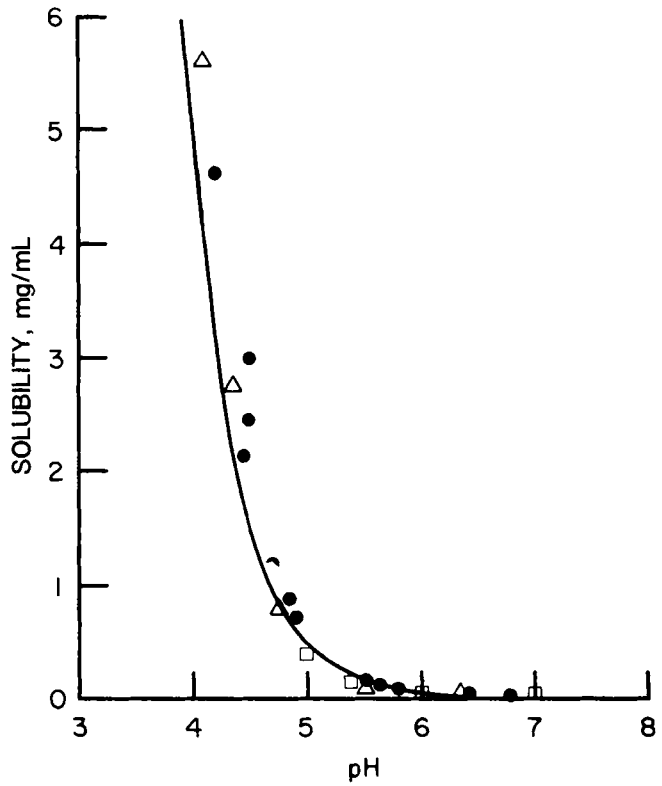

Figure 4—*The solubility of I and II at pH higher than pH_{max} shown with an expanded scale. The solubility was determined by increasing the pH of a solution of I with 1 M NaOH (●), by decreasing the pH of a solution of II with 1 M HCl (△), and by adding II to citric acid-phosphate buffer (□). The solid line was generated theoretically according to Eq. 3.*

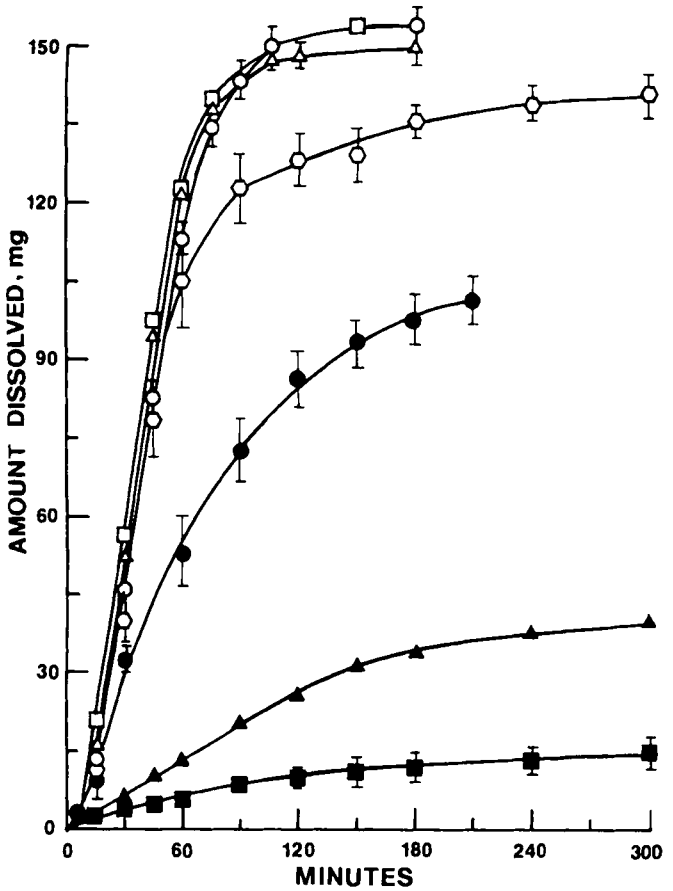

Figure 5 —*Dissolution of I from papaverine sustained-release pellets in citric acid–phosphate buffers. Key: (○) pH 2.2; (△) pH 3; (□) pH 4; (○) pH 5; (●) pH 5.4; (▲) pH 6; (■) pH 7. Each point represents mean ± SD of three experimental values, except for pH 6, for which the mean of duplicate determinations was plotted.*

i.e., equal to the solubility of the salt. The solubility of I, however, dropped gradually on lowering the pH below 2 with the addition of 1 M HCl. The chloride concentrations of solutions with pH values lower than pH_{max} are plotted in Fig. 2. Between pH 2 and 4, the chloride concentration remained constant, along with the constant solubility exhibited over this range (Fig. 1). A sharp increase in chloride ion concentration below pH 2 showed that the decline in solubility in Fig. 1 was due to a common-ion effect.

Solubility in Buffers— The pH–solubility of profile I in citric acid–phosphate buffers is presented in Fig. 3. As in Fig. 1, the apparent pH_{max} was 3.9 (higher than the theoretical pH_{max}), but the solubility of the salt at pH values between 2.2 and 3.9 was higher than that in the unbuffered solutions. Equilibrium solubility determinations in buffer showed no supersaturation effect around the apparent pH_{max}. The increase in solubility, however, over that obtained by the addition of acid or base between pH 3.3 and 3.9 may be due to salt formation with the buffer components. When an excess of I was added to the buffers with an initial pH higher than the apparent pH_{max}, the pH dropped to the latter value. The data points A, B, and C (Fig. 3) were obtained by adding an excess of I to buffers of pH 4, 5, and 5.4, respectively. Since the profile could not be extended below pH 2.2 in the citric acid–phosphate buffer system, no common-ion effect was noticed.

The solubilities above the apparent pH_{max} determined by (*a*) increasing the pH of a solution of I, (*b*) decreasing the pH of a solution of II, and (*c*) adding II to citric acid–phosphate buffer are shown with an expanded scale in Fig. 4. The line drawn is a theoretical value based on Eq. 3. As noted earlier, the solubility below pH 4.6 lies higher than the theoretical line.

Equilibrium solubility values determined by overnight shaking were plotted in Fig. 3, whereas Fig. 1 was generated by titration. An apparent pH_{max} of 3.9 in both cases, which is higher than the value of 3.0 derived theoretically, suggests that the positive deviation in solubility profile observed in Fig. 1 was not due to nonequilibrium conditions. Bogardus and Blackwood (10) have also observed similar nonideal behavior in the pH–solubility profile of doxycycline hydrochloride and have suggested that this might be due to self-association of the solute.

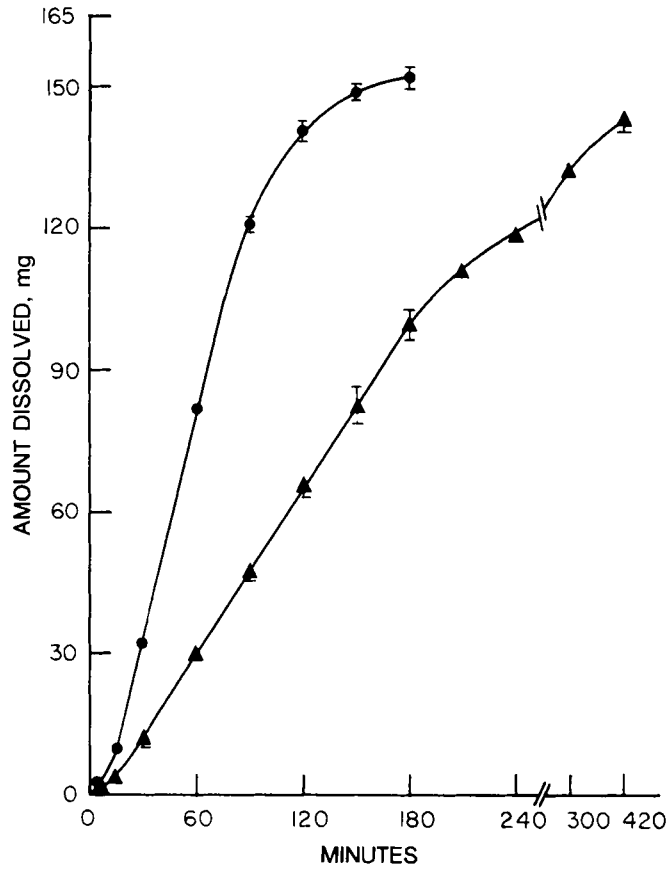

Figure 6—*Dissolution of I from papaverine sustained-release pellets in 0.01 M HCl (●) and 0.1 M HCl (▲). Each point represents mean ± SD of the three experimental values.*

Dissolution from Papaverine Sustained-Release Pellets— The dissolution of I from sustained-release pellets of I in citric acid–phosphate buffers at pH values of 2.2, 3.0, 4.0, 5.0, 5.4, 6.0, and 7.0 is shown in Fig. 5. The graphs in the pH region between 2.2 and 5.0 showed linearity after certain initial lag periods. This implies that the release rates were zero order for the periods corresponding to the linearity. At pH 2.2, 3.0, and 4.0, 100% of the drug was

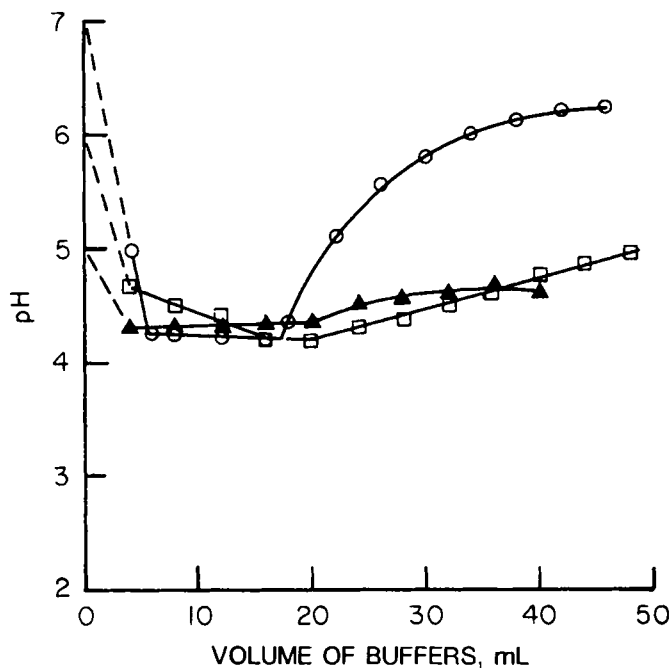

Figure 7— *Changes of pH of citric acid–phosphate buffers added to 1 g of I. Key: (▲) pH 5; (□) pH 6; (○) pH 7.*

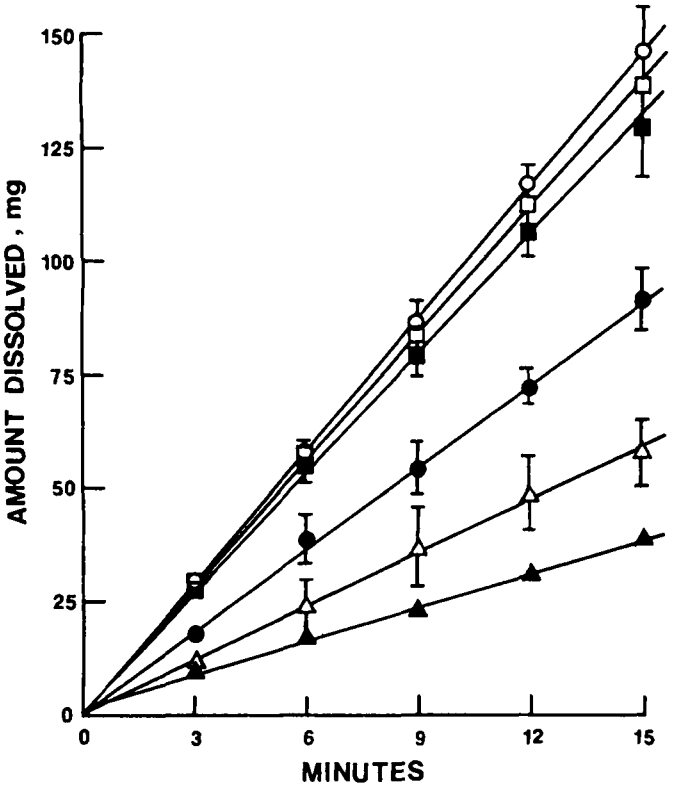

Figure 8—*Dissolution profiles of I from a constant surface area of 0.95 cm^2 at 37°C in various buffers. Each point represents mean ± SD of three experimental values. Key: (▲) pH 1.1; (●) pH 2.0; (○) pH 2.2; (□) pH 4.0; (■) pH 5.0; (△) pH 6.0. Deposition of a porous film of papaverine base was observed on the surface of I at pH 6.0.*

released from the pellets, whereas at pH ≥5.0, the dissolution profiles leveled off before complete release.

The zero-order rates in the pH range between 2.2 and 5.0 were calculated from the straight-line portions of the graphs. The release rates at pH 5.4, 6.0, and 7.0 were calculated from the initial portions of the graphs (<60 min) since sink conditions were not fulfilled. The rate constants, the solubilities, and their ratios at various pH are shown in Table I. According to Fig. 3, the saturation solubility between pH 2.2 and 3.9 was almost constant. This agrees with a similar constancy in dissolution rates at pH 2.2, 3.0, and 4.0. The dissolution of the pellets was also measured in 0.01 and 0.1 M HCl to study the effect of solubility on release rates (Fig. 6, Table I). In these two media, the saturation solubilities were 42 and 20 mg/mL, and the zero-order dissolution rates were 1.6 and 0.6 mg/min, respectively. Thus, at the apparent pH_{max} and lower, the dissolution rates were approximately proportional to the solubilities.

Similar proportional relationships between the solubility and the dissolution rate did not exist at higher pH. For example, although the solubilities at pH 5.0 and 5.4 were 152 and 390 times lower, respectively, than the solubility in the pH range of 2.2–3.9, the dissolution rates decreased only by factors of 1.1 and 2.3. This effect is further illustrated in Table I by the ratios of dissolution rate from pellets to solubility. At pH ≤4, the ratios were very small and almost constant, whereas at higher pH, the ratios were much larger. The discontinuity between the two sets of ratios occurred at the apparent pH_{max}.

Self-Buffering Action of I—The larger dissolution rate to solubility ratio at pH values higher than the apparent pH_{max} may be related to the effect of an excess of I on the pH of the buffer solutions. When buffers of pH 5.0, 6.0, and 7.0 were added to solid drug, the pH always dropped to a level between 4.0 and 4.5 and remained at this level until a considerable excess of buffer was added to raise the pH (Fig. 7). The same effect was also observed when an excess of I in solid form was added to pH 6 buffer, causing the pH to drop to 3.9. As long as an excess of I in solid form was present, the pH of the solution remained between 3.9 and 4.5, although the initial pH values of the buffers were higher. This pH range corresponds to the apparent pH_{max} and the supersaturation range of I (Fig. 1). The self-buffering action of I inside the pellets may increase the effective drug solubility, thus giving higher release rates at external pH values greater than the apparent pH_{max}. The increase in solubility due to the self-buffering action of I may not be identical when buffers of different pH values are used as the dissolution media. This is apparent from Fig. 3, in which points B and C represent the saturation solubilities of I in citric acid–phosphate buffers of pH 5.0 and 5.4, respectively.

The dissolution profiles of I from constant surfaces in selected media are shown in Fig. 8, and the results are tabulated in Table I along with those from sustained-release pellets. The profiles showed apparent linearity, although sink conditions should not exist at pH 5.0 and 6.0. According to the Noyes–Whitney equation (11), the dissolution rate (J) of a compound is proportional to the saturation solubility (C_s), and J/C_s is constant if the surface area, diffusion layer thickness, and diffusion coefficient are assumed to be constant. However, due to the self-buffering action in the diffusion layer (12, 13), the intrinsic dissolution rates of I at pH > pH_{max} were not proportional to the solubilities. This similarity with the dissolution from pellets confirms that the self-buffering action of I was involved in the dissolution from sustained-release pellets.

Mechanism of Release from Sustained-Release Pellets—The linearity of the drug release with time and the extended duration indicate zero-order kinetics for the dissolution rate. The structure of the pellets, consisting of I dispersed in a matrix of shellac with added filler, suggests a mechanism involving the leaching of the drug from the matrix (14). The equation describing the heterogeneous diffusion-controlled matrix model is:

$$Q = \left[\frac{D\epsilon C_s}{\tau}(2A - \epsilon C_s)t\right]^{1/2} \qquad \text{(Eq. 4)}$$

where Q is the amount of drug released per unit area from a matrix of porosity ϵ, tortuosity τ, and initial drug concentration A at the time t. D and C_s are the diffusion coefficient and solubility of the drug in the permeating solvent, respectively. Figure 9a and b show photomicrographs of the cross sections of pellets. The diameter of the core is ~0.6 mm, as compared with the diameter of 0.9 mm for the pellet. The outermost layer produced by the addition of shellac and filler cannot be clearly identified in Fig. 9a, because slight migration of I to this layer during spraying of the shellac solution obscures the distinction under UV light. However, the outermost barrier layer is distinguishable and remains intact after total leaching of I (Fig. 9b); the thickness of this layer is estimated to be 20–30 μm. From the core volume and papaverine hydrochloride charge, A was estimated at 700 mg/mL, and the condition $A \gg C_s$ was satisfied. Porosimetry measurements of pellets allowed computation of the average porosity of the penetrated portion of the matrix, which

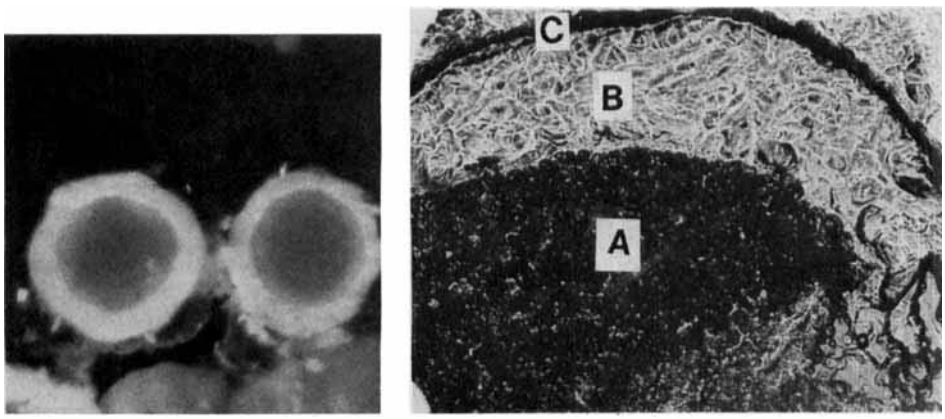

Figure 9—*Photomicrographs of (a) cross-sections of gross pellets (magnification, 30×) showing internal sugar beads and fluorescence of the papaverine hydrochloride annulus and (b) microtomed cross sections of leached-out pellets (magnification, 100×). Key: (A) sugar core; (B) leached-out annulus filled with paraffin; (C) outer shellac-filled layer.*

was ~0.6[14]. The tortuosity term must be high, particularly since additional shellac and filler were added in the final stages of pellet preparation. From the dissolution rate of pellets without added filler, a value of 30 was estimated for τ by Eq. 4. By assuming from the pellet core dimensions a matrix thickness of 150 μm and a boundary layer thickness of 100 μm, the ratio of resistances of matrix to unstirred layer is of the order of ~75, so matrix-controlled release proportional to $t^{1/2}$ would be predicted. The zero-order release rates that were observed, however, imply a constant activity of drug in a reservoir, due possibly to a barrier layer on the surface of the pellet where a constant concentration is maintained. Diffusion at constant concentrations through such a barrier layer may be the rate-determining step which results in release being linear with time. This mechanism was confirmed by dissolution from thick films of I dispersed in a shellac-based matrix in the same proportion as in the pellets but without the final drug-free layer. The release was found to be linear with $t^{1/2}$ and agreed with the heterogeneous matrix model. Moreover, the release from pellets made without the outer layer of shellac and filler also adhered to the $t^{1/2}$ relationship.

The sensitivity of the release rates to pH of the external solvent at pH < pH_{max} confirms that the leaching process takes place within a granular matrix. However, the expected decrease of release rate based on the decreased solubility at higher pH was not observed. These results were explained by the self-buffering action of the drug and the tendency to revert toward the apparent pH_{max} in the media of low buffer capacity.

The results of the present investigation indicate that the variability in the dissolution rate of a drug within the GI pH range due to differences in solubility may be reduced by designing controlled-release dosage forms. The importance of internal pH within the polymer matrices in controlling the solubility of drug and hence the dissolution rate has also been noted by Jambhekar and Cobby (15).

[14] The maximum porosity when all of the active drug is dissolved is given by $\epsilon + A(1 - \epsilon)$, where ϵ is the porosity of the pellet equal to 0.07, and A is the concentration of drug in the matrix.

REFERENCES

(1) R. J. Timko and N. G. Lordi, *J. Pharm. Sci.*, **67,** 496 (1978).
(2) S. F. Kramer and G. L. Flynn, *J. Pharm. Sci.*, **61,** 1896 (1972).
(3) Z. T. Chowhan, *J. Pharm. Sci.*, **67,** 1257 (1978).
(4) M. Robinson, in "The Theory and Practice of Industrial Pharmacy," 2nd ed., L. Lachman, H. A. Lieberman, and J. L. Kanig, Eds., Lea & Febiger, Philadelphia, Pa., 1976, p. 456.
(5) L. W. Dittert, T. Higuchi, and D. R. Reese, *J. Pharm. Sci.*, **53,** 1325 (1964).
(6) I. M. Kolthoff, *Biochem. Z.*, **162,** 289 (1925).
(7) V. H. Veley, *J. Chem. Soc.*, **95,** 758 (1909).
(8) A. I. Biggs, *Trans. Faraday Soc.*, **50,** 800 (1954).
(9) J. H. Wood, J. E. Syarto, and H. Letterman, *J. Pharm. Sci.*, **54,** 1068 (1965).
(10) J. B. Bogardus and R. K. Blackwood, *J. Pharm. Sci.*, **68,** 188 (1979).
(11) A. A. Noyes and W. R. Whitney, *J. Am. Chem. Soc.*, **19,** 930 (1897).
(12) E. Nelson, *J. Am. Pharm. Assoc., Sci. Ed.*, **46,** 607 (1957).
(13) K. G. Mooney, M. A. Mintun, K. J. Himmelstein, and V. J. Stella, *J. Pharm. Sci.*, **70,** 13 (1981).
(14) T. Higuchi, *J. Pharm. Sci.*, **52,** 1145 (1963).
(15) S. Jambhekar and J. Cobby, Abstracts, Academy of Pharmaceutical Sciences 29th National Meeting, **10**(2), 86 (1980).

ACKNOWLEDGMENTS

The authors wish to thank Mr. J. Breitbart for measurements of the dissolution rates of papaverine hydrochloride from films and Dr. D. Mufson for his encouragement and advice throughout the course of this study and for critical review of the manuscript.

Serum and Myocardial Kinetics of Amiodarone and Its Deethyl Metabolite After Intravenous Administration in Rabbits

R. KANNAN *x, N. IKEDA ‡, R. WAGNER ‡, M. DRACHENBERG ‡, and B. N. SINGH *

Received July 5, 1983, from the **Department of Cardiology, Veterans Administration Medical Center, West Los Angeles, CA 90073* and the ‡*Department of Medicine, UCLA School of Medicine, Los Angeles, CA.* Accepted for publication October 6, 1983.

Abstract □ The serum kinetics of amiodarone and its major metabolite the deethyl analogue were studied in rabbits after intravenous administration. The elimination of the drug and the metabolite from serum occurred as a biexponential function. Both compounds exhibited a rapid distribution phase (6.5 and 4.4 min, respectively) and had elimination half-lives of 136 and 235 min, respectively. There was a rapid uptake of both drugs by the myocardium, with maximal concentrations at 5 and 15 min. The myocardial concentrations were higher than the respective serum concentrations and declined with time. There was a wide scatter in myocardium-serum ratios, which ranged from 1 to 11 for amiodarone and 12 to 29 for the metabolite. Neither the drug nor the metabolite produced significant changes in the surface electrocardiogram after intravenous administration. These data suggest that accumulation of the metabolite does not account for the slow onset of action of amiodarone.

Keyphrases □ Kinetics—serum and myocardial, amiodarone and its metabolite, rabbits □ Amiodarone—serum and myocardial kinetics, rabbits □ Deethyl metabolite—amiodarone, serum and myocardial kinetics, rabbits

Plasma drug levels are commonly used to monitor the efficacy and toxicity of antiarrhythmic compounds. Such an approach is based on the assumption that the drug level in the myocardium, the presumed site of action of cardioactive agents, is in equilibrium with that in plasma. However, this assumption may not necessarily be valid under conditions of rapidly changing plasma levels of drugs (1). The significance of the myocardium–plasma drug ratios in the interpretation of the pharmacological responses of antidysrhythmic agents such as lidocaine (2), quinidine (3), verapamil (4), disopyramide (5), and *n*-acetylprocainamide (6) has been emphasized. Such studies are particularly relevant in the case of amiodarone, a potent class III antiarrhythmic drug (7), in light of our recent finding which demonstrates a lack of correlation between serum drug concentrations and suppression of premature ventricular contractions in patients with cardiac arrhythmias (8). Chronic amiodarone therapy results in the accumulation of a metabolite, the deethyl analogue, in serum (9). However, neither the pharmacokinetics nor the pharma-

0022-3549/84/0900-1208$01.00/0